2015 American Control Conference
Palmer House Hilton
July 1-3, 2015. Chicago, IL, USA

Nonlinear Dynamics of Connected Vehicle Systems with Communication Delays

Linjun Zhang and Gábor Orosz

Abstract— **In this paper, we investigate effects of communication delays on the nonlinear dynamics of connected vehicle systems. Our modeling framework incorporates communication delays, which arise from the intermittency and packet drops in wireless vehicle-to-vehicle communication. Plant stability and string stability are used to characterize the system-level performance of vehicle networks. Delay-dependent stability conditions are derived based on the Lyapunov-Krasovskii theorem and then visualized by using stability diagrams. Numerical simulations are used to validate the stability diagrams and to demonstrate that bistability can be avoided by utilizing the nonlinear stability analysis presented in this paper.**

I. INTRODUCTION

In recent years, cooperative adaptive cruise control (CACC) has been intensively studied and showed great potentials in improving traffic efficiency [1]–[3]. CACC requires that each vehicle monitors the motion of the vehicle immediately ahead by range sensors (e.g., radar) as well as the motion of the designated leader via wireless vehicle-to-vehicle (V2V) communication. Such fixed connectivity structure does not take full advantage of V2V communication and also makes it difficult to implement CACC in real traffic, where most of vehicles are not equipped with radar.

To fully exploit V2V communication, connected cruise control (CCC) was proposed [4]–[7], which allows one to utilize ad-hoc connections with multiple vehicles ahead. CCC can be used either to assist human drivers or to automatically regulate the longitudinal motion of vehicles. Incorporating CCC vehicles into the flow of non-CCC vehicles leads to connected vehicle systems (CVSs), which require neither designated leader nor fixed connectivity structure. Since CVSs allow the incorporation of human-driven vehicles that are not equipped with range sensors or V2V communication devices, it can be implemented in real traffic.

Plant stability and string stability are typically used to characterize the system-level performance of vehicle networks [8], [9]. Plant stability requires that the equilibrium of all vehicles in the network is asymptotically stable in absence of external disturbances. If some vehicles cause disturbances by accelerating or decelerating, the vehicle network is said to be string stable if the disturbances are attenuated when propagating upstream. In [4], the stability of CVSs was investigated by using linearized models. Thus, the corresponding results are only valid in the vicinity of the equilibrium.

The nonlinear dynamics of CVSs were studied in [10] by neglecting information delays that may indeed influence the stability significantly. In this paper, we investigate the effects of information delays on the nonlinear dynamics of CVSs. Considering that delay-independent stability conditions are typically quite conservative, we seek for delay-dependent conditions for plant stability and string stability by using the Lyapunov-Krasovskii theory. Compared with the results obtained using linearized models, the stability conditions derived in this paper are more robust against large disturbances.

The rest of this paper is organized as follows. A general framework for CCC design is presented in Section II, which incorporates the information delays and nonlinear range policies. In Section III, we derive the delay-dependent stability conditions for plant stability and head-to-tail string stability of a CCC cascade. The stability diagrams and simulations in Section IV demonstrate that the bistability caused by large perturbations can be avoided using the nonlinear stability analysis presented in this paper. Finally, conclusions are presented in Section V.

II. DYNAMICS AND STABILITY OF CONNECTED VEHICLE SYSTEMS

In this section, a framework is presented for modeling the longitudinal dynamics of vehicles equipped with connected cruise control (CCC), which utilize motion data received from multiple vehicles ahead via wireless vehicle-to-vehicle (V2V) communication. We incorporate the information delays that arise due to intermittency and packet drops in V2V communication. This framework ensures the existence of uniform flow equilibrium in the resulting connected vehicle systems (CVSs), which is independent of the network size, connectivity structure, information delays, and control gains.

A. Dynamics of Connected Cruise Control

Fig. 1 demonstrates a scenario where the CCC vehicle i monitors the positions and velocities of vehicles $j = p,\dots,i-1$, where p denotes the furthest vehicle that vehicle i can monitor due to the limitation of effective communication range. Note that vehicle p is not necessarily the head vehicle of the network. Here, h_j denotes the distance between vehicle $j-1$ and vehicle j, which is also called headway, and v_j is the speed of vehicle j. Moreover, $\xi_{i,j}$ represents the delay for vehicle i receiving motion data from vehicle j, and $\xi_{i,j}$ may be human reaction time (0.5–1.5 [s]), sensing delay (0.1–0.2 [s]), or communication delay (0.1–0.4 [s]).

This work was supported by the National Science Foundation (Award Number 1351456)

The authors are both with the Department of Mechanical Engineering, the University of Michigan, Ann Arbor, MI, 48109, USA linjunzh@umich.edu, orosz@umich.edu

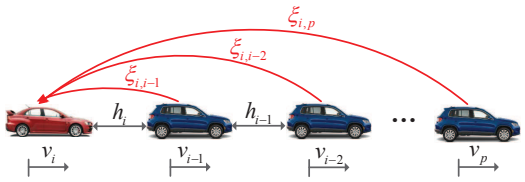

Fig. 1. A vehicle network where a CCC vehicle (red) at the tail receives information from multiple vehicles ahead. Other vehicles (blue) may be either CCC or non-CCC vehicles. The symbols h_j and v_j denote the headway and the speed of vehicle j, respectively, while $\xi_{i,j}$ denotes the information delay between vehicles i and j.

We use the CCC framework presented in [4], that is, the car-following dynamics of the CCC vehicle i is governed by

$$\begin{aligned} \dot{h}_i(t) &= v_{i-1}(t) - v_i(t)\,, \\ \dot{v}_i(t) &= \sum_{j=p}^{i-1} \alpha_{i,j}\big(V_i\big(\bar{h}_{i,j}(t-\xi_{i,j})\big) - v_i(t-\xi_{i,j})\big) \\ &\quad + \sum_{j=p}^{i-1} \beta_{i,j}\big(v_j(t-\xi_{i,j}) - v_i(t-\xi_{i,j})\big)\,, \end{aligned} \tag{1}$$

where constants $\alpha_{i,j}$ and $\beta_{i,j}$ are control gains, and $V_i(h)$ denotes the range policy that gives the desired speed as a function of headway h. The quantity

$$\bar{h}_{i,j} = \frac{1}{i-j}\sum_{k=j+1}^{i} h_k \tag{2}$$

denotes the average headway between vehicles i and j, which is used to make the equilibrium independent of network size while enabling comparison of desired speeds obtained for different j's. When all vehicles utilize the same range policy, i.e., $V_i(h) = V(h)$ for all i, the framework (1) guarantees the existence of a unique uniform flow equilibrium

$$h_i(t) \equiv h^*\,, \quad v_i(t) \equiv v^* = V(h^*)\,, \tag{3}$$

for all i, which is independent of network size, connectivity structures, information delays, and control gains. If vehicles use different range policies, the equilibrium still exists but not in uniform. That is, $h_i(t) \equiv h_i^*$ and $v_i(t) \equiv v^* = V(h_i^*)$ but $h_i^* \neq h_j^*$ for $i \neq j$. Since traffic data indicate that the equilibrium is typically close to uniform [11], we neglect such heterogeneities for simplicity.

In this paper, we utilize the range policy function

$$V(h) = \begin{cases} 0\,, & \text{if} \quad h \le h_{\rm st}\,, \\ \frac{v_{\max}}{2}\left[1 - \cos\left(\pi \frac{h-h_{\rm st}}{h_{\rm go}-h_{\rm st}}\right)\right], & \text{if} \quad h_{\rm st} < h < h_{\rm go}\,, \\ v_{\max}\,, & \text{if} \quad h \ge h_{\rm go}\,. \end{cases} \tag{4}$$

This indicates that for small headways $h \le h_{\rm st}$, the vehicle tends to stop for safety reasons. For large headways $h \ge h_{\rm go}$, the vehicle aims to maintain the preset maximum speed $v_{\max}$. Between $h_{\rm st}$ and $h_{\rm go}$, the desired velocity monotonically increases with the headway. The nonlinear function for $h_{\rm st} < h < h_{\rm go}$ in (4) ensures the smooth change of acceleration at $h = h_{\rm st}$ and $h = h_{\rm go}$ and hence improves the driving comfort. According to the data collected in real traffic [11], parameters in (4) are set as $h_{\rm st} = 5$ [m], $h_{\rm go} = 35$ [m], $v_{\max} = 30$ [m/s].

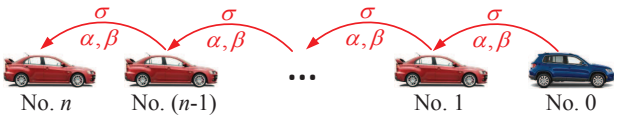

Fig. 2. CCC cascade where all followers are CCC vehicles that only react to the vehicle immediately ahead. The symbol σ denotes the communication delay while the control gains are given by α and β.

B. Plant Stability and String Stability

Plant stability and string stability are used to characterize the system-level performance of vehicle networks. Plant stability indicates that, in absence of external disturbances, the uniform flow equilibrium (3) is asymptotically stable. Head-to-tail string stability means that the disturbances caused by the head vehicle are decreased when reaching the tail vehicle, allowing that disturbances may be amplified by some vehicles in the network. Head-to-tail string stability is particularly useful for CVSs that include human-driven vehicles, as their dynamics cannot be designed and hence may amplify the disturbances.

Suppose that the velocity of vehicle i is expressed by $v_i(t) = v^* + \tilde{v}_i(t)$ for $i = 0, 1, \ldots$, where the equilibrium velocity v^* is given by (3) while $\tilde{v}_i(t)$ denotes the perturbation about the equilibrium. There are many ways to evaluate the head-to-tail string stability depending on what disturbances to consider and how to characterize the magnitude of the signals. Considering that disturbance signals may be expressed by using Fourier series where each element is a sinusoidal term, we use the sinusoidal disturbance

$$\tilde{v}_0(t) = v_{\rm amp}\sin(\omega t)\,, \tag{5}$$

where $v_{\rm amp}, \omega \in \mathbb{R}_+$ denote the amplitude and the frequency of the disturbance, respectively. Moreover, we use the $\mathscr{L}_\infty$-norm to evaluate the magnitude of signals, i.e., $\|\tilde{v}\|_\infty = \sup_{t>0}|\tilde{v}(t)|$. Then, a vehicle network is said to be head-to-tail string stable if

$$\|\tilde{v}_{ns}\|_\infty \le \|\tilde{v}_0\|_\infty\,, \quad \forall \omega \in \mathbb{R}_+\,, \tag{6}$$

where $\tilde{v}_{ns}$ denotes the steady-state disturbances for the velocity of the tail vehicle.

III. STABILITY OF THE CCC CASCADE

In this section, we study the nonlinear dynamics of a CCC cascade, which is a simple connected vehicle network where all following vehicles are CCC vehicles that only react to the motion of the vehicle immediately ahead via V2V communication, as depicted in Fig. 2. We assume that all CCC vehicles have identical communication delay σ and also use the same control gains α and β. Then, the dynamic model of the CCC cascade is given by

$$\begin{aligned} \dot{h}_i(t) &= v_{i-1}(t) - v_i(t)\,, \\ \dot{v}_i(t) &= \alpha\big(V\big(h_i(t-\sigma)\big) - v_i(t-\sigma)\big) \\ &\quad + \beta\big(v_{i-1}(t-\sigma) - v_i(t-\sigma)\big)\,, \end{aligned} \tag{7}$$

for $i=1,\dots,n$; cf. (1). We define perturbations about the equilibrium (3) as

$$\tilde{h}_i(t)=h_i(t)-h^*\,,\quad \tilde{v}_i(t)=v_i(t)-v^*=v_i(t)-V(h^*)\,, \tag{8}$$

for $i=1,\dots,n$. Substituting (8) into (7) yields

$$\begin{aligned}\dot{\tilde{h}}_i(t)&=\tilde{v}_{i-1}(t)-\tilde{v}_i(t)\,,\\ \dot{\tilde{v}}_i(t)&=\alpha\big(V\big(h_i(t-\sigma)\big)-V(h^*)-\tilde{v}_i(t-\sigma)\big)\\ &\quad+\beta\big(\tilde{v}_{i-1}(t-\sigma)-\tilde{v}_i(t-\sigma)\big)\,.\end{aligned} \tag{9}$$

We assume bounded headways $h_i\in\mathscr{D}\subseteq\mathbb{R}_+$, which implies bounded equilibrium headway $h^*\in\mathscr{D}$. Then, based on the mean value theorem, there exists $\psi_i\in\mathscr{D}$ such that

$$V\big(h_i(t-\sigma)\big)-V(h^*)=V'(\psi_i)\tilde{h}_i(t-\sigma)\,, \tag{10}$$

where the prime denotes differentiation with respect to h and ψ_i is an explicit function of $\tilde{h}_i$; cf. (4). Substituting (10) into (9) and writing the results in the matrix form, we obtain

$$\begin{aligned}\dot{x}_i(t)&=A_0x_i(t)+A_\sigma(\psi_i)x_i(t-\sigma)\\ &\quad-A_0x_{i-1}(t)+Bx_{i-1}(t-\sigma)\,,\end{aligned} \tag{11}$$

for $i=1,\dots,n$, where matrices are given by

$$\begin{aligned}x_i(t)&=\begin{bmatrix}\tilde{h}_i(t)\\ \tilde{v}_i(t)\end{bmatrix}, & A_0&=\begin{bmatrix}0&-1\\0&0\end{bmatrix},\\ A_\sigma(\psi_i)&=\begin{bmatrix}0&0\\ \varphi(\psi_i)&-\kappa\end{bmatrix}, & B&=\begin{bmatrix}0&0\\0&\beta\end{bmatrix},\end{aligned} \tag{12}$$

and

$$\varphi(\psi_i)=\alpha V'(\psi_i)\,,\quad \kappa=\alpha+\beta\,. \tag{13}$$

Note that (11) is equivalent to the nonlinear model (9) since no approximations are used throughout the process.

A. Plant Stability

When analyzing the plant stability, we neglect perturbations from other vehicles, i.e., $\tilde{x}_{i-1}(t)\equiv 0$ in (11), yielding an autonomous nonlinear delayed system

$$\dot{x}_i(t)=A_0x_i(t)+A_\sigma(\psi_i)x_i(t-\sigma)\,. \tag{14}$$

Applying the Newton-Leibniz formula leads to

$$x_i(t-\sigma)=x_i(t)-\int_{t-\sigma}^{t}\dot{x}_i(r)\,\mathrm{d}r\,. \tag{15}$$

Substituting (15) into (14) results in

$$\dot{x}_i(t)=A(\psi_i)x_i(t)-A_\sigma(\psi_i)\int_{t-\sigma}^{t}\dot{x}_i(r)\,\mathrm{d}r\,, \tag{16}$$

where

$$A(\psi_i)=A_0+A_\sigma(\psi_i)\,. \tag{17}$$

In the rest of this paper, we use $L\succ 0$ to denote that a quantity L is positive definite and use $L\prec 0$ to denote a negative definite quantity L. Then, a delay-dependent sufficient condition for the plant stability of the CCC cascade (7) is given by the following theorem.

Theorem 1: For delay σ and domain $h_i\in\mathscr{D}$ $(i=1,\dots,n)$, the CCC cascade (7) is plant stable if there exist constant symmetric matrices $P,Q,W\succ 0$ such that

$$\Omega(\psi_i)=\begin{bmatrix}\frac{A^{\mathrm{T}}P+PA+Q+\sigma A_0^{\mathrm{T}}WA_0}{\sigma} & A_0^{\mathrm{T}}WA_\sigma & -PA_\sigma\\ A_\sigma^{\mathrm{T}}WA_0 & \frac{\sigma A_\sigma^{\mathrm{T}}WA_\sigma-Q}{\sigma} & \mathbf{0}_{2\times 2}\\ -A_\sigma^{\mathrm{T}}P & \mathbf{0}_{2\times 2} & -W\end{bmatrix}\prec 0 \tag{18}$$

holds for $\forall\psi_i\in\mathscr{D}$, where arguments of $A_\sigma(\psi_i)$ and $A(\psi_i)$ are not spelled out to save space.

Proof: To prove Theorem 1, we utilize the Lyapunov-Krasovskii stability theorem [12] by using the functional

$$\begin{aligned}L&=x_i^{\mathrm{T}}(t)Px_i(t)+\int_{t-\sigma}^{t}x_i^{\mathrm{T}}(r)Qx_i(r)\,\mathrm{d}r\\ &\quad+\int_{-\sigma}^{0}\int_{t+\theta}^{t}\dot{x}_i^{\mathrm{T}}(r)W\dot{x}_i(r)\,\mathrm{d}r\,\mathrm{d}\theta\,,\end{aligned} \tag{19}$$

where $P,Q,W\succ 0$ yields $L\succ 0$.

Differentiating (19) with respect to time and using (14) and (16), we obtain

$$\begin{aligned}\dot{L}&=X_i^{\mathrm{T}}(t)\Phi(\psi_i)X_i(t)-2x_i^{\mathrm{T}}(t)PA_\sigma\int_{t-\sigma}^{t}\dot{x}_i(r)\,\mathrm{d}r\\ &\quad-\int_{t-\sigma}^{t}\dot{x}_i^{\mathrm{T}}(r)W\dot{x}_i(r)\,\mathrm{d}r\,,\end{aligned} \tag{20}$$

where $X_i^{\mathrm{T}}(t)=[x_i^{\mathrm{T}}(t),\ x_i^{\mathrm{T}}(t-\sigma)]$ and

$$\Phi(\psi_i)=\begin{bmatrix}A^{\mathrm{T}}P+PA+Q+\sigma A_0^{\mathrm{T}}WA_0 & \sigma A_0^{\mathrm{T}}WA_\sigma\\ \sigma A_\sigma^{\mathrm{T}}WA_0 & \sigma A_\sigma^{\mathrm{T}}WA_\sigma-Q\end{bmatrix}. \tag{21}$$

Considering the identity

$$X_i^{\mathrm{T}}(t)\Phi(\psi_i)X_i(t)=\frac{1}{\sigma}\int_{t-\sigma}^{t}X_i^{\mathrm{T}}(t)\Phi(\psi_i)X_i(t)\,\mathrm{d}r \tag{22}$$

in (20) yields

$$\dot{L}=\int_{t-\sigma}^{t}\chi_i^{\mathrm{T}}(t,r)\Omega(\psi_i)\chi_i(t,r)\,\mathrm{d}r\,, \tag{23}$$

where $\chi_i^{\mathrm{T}}(t,r)=[x_i^{\mathrm{T}}(t)\,,\ x_i^{\mathrm{T}}(t-\sigma)\,,\ \dot{x}_i^{\mathrm{T}}(r)]$ and $\Omega(\psi_i)$ is given by (18). If (18) holds, we have $\chi_i^{\mathrm{T}}(t,r)\Omega(\psi_i)\chi_i(t,r)\prec 0$ for $r\in[t-\sigma,\ t]$. Since the integration does not change the negative sign, we have $\dot{L}\prec 0$, implying that the equilibrium $x_i=0$ $(i=1,\dots,n)$ is asymptotically stable. ■

We emphasize that the condition (18) leads to the largest stable domain that can be obtained by the Lyapunov-Krasovskii functional (19), since neither inequalities nor approximations are used throughout the derivation. For given domain $\mathscr{D}$, the plant stability condition (18) can be numerically solved for P,Q,W by utilizing linear matrix inequality (LMI) toolbox in MATLAB for sufficiently many points in $\mathscr{D}$. The corresponding results are visualized in stability diagrams as shown in Section IV.

B. Head-to-Tail String Stability

Considering that string stability is used to characterize the steady-state performance under periodic excitations, we begin by presenting a condition that ensures the existence of periodic steady-state response.

Theorem 2: Suppose that the disturbance on the speed of head vehicle is T-periodic. If Theorem 1 holds, then the CCC cascade (7) has T-periodic steady-state response, i.e.,

$$x_{is}(t+T) = x_{is}(t), \quad i = 1, \dots, n, \tag{24}$$

where the subscript "s" denotes the steady state.

Proof: Substituting $t = t+T$ into (9) for $i = 1$, subtracting (9), and considering the periodicity $\tilde{v}_0(t+T) = \tilde{v}_0(t)$ and $\tilde{v}_0(t+T-\sigma) = \tilde{v}_0(t-\sigma)$, we have

$$\begin{aligned} \dot{\tilde{h}}_1(t+T) - \dot{\tilde{h}}_1(t) &= -\big(\tilde{v}_1(t+T) - \tilde{v}_1(t)\big), \\ \dot{\tilde{v}}_1(t+T) - \dot{\tilde{v}}_1(t) &= \alpha\big(V\big(h_1(t+T-\sigma)\big) - V\big(h_1(t-\sigma)\big)\big) \\ &\quad - \kappa\big(\tilde{v}_1(t+T-\sigma) - \tilde{v}_1(t-\sigma)\big). \end{aligned} \tag{25}$$

For $h_i \in \mathscr{D}$, based on the mean value theorem, there exists $\mu_i \in \mathscr{D}$ such that

$$\begin{aligned} &V\big(h_i(t+T-\sigma)\big) - V\big(h_i(t-\sigma)\big) \\ =&V'(\mu_i)\big(\tilde{h}_i(t+T-\sigma) - \tilde{h}_i(t-\sigma)\big), \end{aligned} \tag{26}$$

for $i = 1, \dots, n$. Note that μ_i is a function of $\tilde{h}_i$; cf. (10). We define the error $e_1(t) = x_1(t+T) - x_1(t)$, substitute (26) into (25), and write the result in matrix form, which yields

$$\begin{aligned} \dot{e}_1(t) &= A_0 e_1(t) + A_\sigma(\mu_1) e_1(t-\sigma) \\ &= A(\mu_1) e_1(t) - A_\sigma(\mu_1) \int_{t-\sigma}^{t} \dot{e}_1(r)\,\mathrm{d}r, \end{aligned} \tag{27}$$

cf. (14) and (16).

With the same $P, Q, W \succ 0$ as used in Theorem 1, the Lyapunov-Krasovskii functional becomes

$$\begin{aligned} L = e_1^{\mathrm{T}}(t) P e_1(t) &+ \int_{t-\sigma}^{t} e_1^{\mathrm{T}}(r) Q e_1(r)\,\mathrm{d}r \\ &+ \int_{-\sigma}^{0} \int_{t+\theta}^{t} \dot{e}_1^{\mathrm{T}}(r) W \dot{e}_1(r)\,\mathrm{d}r\mathrm{d}\theta, \end{aligned} \tag{28}$$

while its time derivative is given by

$$\dot{L} = \int_{t-\sigma}^{t} E_1^{\mathrm{T}}(t,r)\,\Omega(\mu_1) E_1(t,r)\,\mathrm{d}r, \tag{29}$$

where $E_1^{\mathrm{T}}(t,r) = [e_1^{\mathrm{T}}(t),\ e_1^{\mathrm{T}}(t-\sigma),\ \dot{e}_1^{\mathrm{T}}(r)]$ and $\Omega(\mu_1)$ is given by (18) while replacing ψ_1 by μ_1. Thus, (18) ensures that $\Omega(\mu_1) \prec 0$ for $\forall \mu_1 \in \mathscr{D}$. Hence, we have $L \succ 0$ and $\dot{L} \prec 0$, implying that $e_1(t) \to 0$ as $t \to \infty$. This leads to zero steady-state error $e_{1\mathrm{s}}(t) \equiv 0$, i.e., $x_{1\mathrm{s}}(t+T) = x_{1\mathrm{s}}(t)$. Based on the results for vehicle 1, one can repeat the aforementioned process for vehicles $2, \dots, n$ and complete the proof for Theorem 2. ∎

When evaluating head-to-tail string stability, we assume sinusoidal disturbance on the speed of head vehicle as given by (5). Since $\tilde{v}_0(t)$ is periodic with period $T = 2\pi/\omega$, based on Theorem 2, a periodic steady state of the CCC cascade (7) exists with the same period. However, due to nonlinearities in the dynamics, the steady states are not purely sinusoidal but may be expressed using the Fourier series.

To analyze string stability, the steady state of the tail vehicle is needed. However, it may not be obtained explicitly due to nonlinearities and delay effects. Thus, we seek for the approximation of the steady state by applying the third-order Taylor expansion to (7) about the equilibrium (3), yielding

$$\begin{aligned} \dot{\tilde{h}}_i(t) &= \tilde{v}_{i-1}(t) - \tilde{v}_i(t), \\ \dot{\tilde{v}}_i(t) &= \varphi^* \tilde{h}_i(t-\sigma) - \kappa \tilde{v}_i(t-\sigma) + \beta \tilde{v}_{i-1}(t-\sigma) \\ &\quad + \alpha\big(\varepsilon \tilde{h}_i^2(t-\sigma) + \delta \tilde{h}_i^3(t-\sigma)\big), \end{aligned} \tag{30}$$

where

$$\varphi^* = \alpha V'(h^*), \quad \varepsilon = \frac{V''(h^*)}{2}, \quad \delta = \frac{V'''(h^*)}{6}. \tag{31}$$

cf. (13).

The steady-state solutions of (30) can be expressed by $\tilde{h}_{is}(t, \varepsilon, \delta)$ and $\tilde{v}_{is}(t, \varepsilon, \delta)$. Applying the first order Taylor expansion with respect to ε and δ yields

$$\begin{aligned} \tilde{h}_{is}(t, \varepsilon, \delta) &= \tilde{h}_{i,1}(t) + \varepsilon \tilde{h}_{i,2}(t) + \delta \tilde{h}_{i,3}(t), \\ \tilde{v}_{is}(t, \varepsilon, \delta) &= \tilde{v}_{i,1}(t) + \varepsilon \tilde{v}_{i,2}(t) + \delta \tilde{v}_{i,3}(t), \end{aligned} \tag{32}$$

for $i = 1, \dots, n$. According to (5), for vehicle 0 we have

$$\tilde{v}_{0,1}(t) = v_{\mathrm{amp}} \sin(\omega t), \quad \tilde{v}_{0,2}(t) = \tilde{v}_{0,3}(t) = 0. \tag{33}$$

Substituting (32) into (30) and matching coefficients of ε and δ, respectively, we obtain

$$\begin{aligned} \dot{\tilde{h}}_{i,j}(t) &= \tilde{v}_{i-1,j}(t) - \tilde{v}_{i,j}(t), \\ \dot{\tilde{v}}_{i,j}(t) &= \varphi^* \tilde{h}_{i,j}(t-\sigma) - \kappa \tilde{v}_{i,j}(t-\sigma) + \beta \tilde{v}_{i-1,j}(t-\sigma) \\ &\quad + \gamma_j \alpha\big(h_{i,1}(t-\sigma)\big)^j, \end{aligned} \tag{34}$$

for $i = 1, \dots, n$ and $j = 1, 2, 3$. Here, $\gamma_1 = 0$ and $\gamma_2 = \gamma_3 = 1$.

First, we consider $j = 1$ in (34), which is a linear time-invariant (LTI) system with excitation $\tilde{v}_{0,1}(t)$ given in (33). Thus, the steady states of (34) for $j = 1$ are in the form

$$\begin{aligned} \tilde{h}_{i,1}(t) &= a_{i,1} \cos(\omega t) + b_{i,1} \sin(\omega t), \\ \tilde{v}_{i,1}(t) &= c_{i,1} \cos(\omega t) + d_{i,1} \sin(\omega t), \end{aligned} \tag{35}$$

where $a_{i,1}, b_{i,1}, c_{i,1}, d_{i,1} \in \mathbb{R}$ are constants. For compactness, we use the coefficient vector

$$z_{i,1} = \begin{bmatrix} a_{i,1} & b_{i,1} & c_{i,1} & d_{i,1} \end{bmatrix}^{\mathrm{T}}. \tag{36}$$

Substituting (35) into (34) for $j = 1$ and matching coefficients of $\cos(\omega t)$ and $\sin(\omega t)$, respectively, we obtain

$$z_{i,1} = \big(C(\omega)\big)^{-1} D_{i,1}, \tag{37}$$

with

$$\begin{aligned} C(\omega) &= \begin{bmatrix} \omega E & I_2 \\ -\varphi^* F(\omega\sigma) & \omega E + \kappa F(\omega\sigma) \end{bmatrix}, \\ D_{i,1} &= \big(B \otimes F(\omega\sigma) - A_0 \otimes I_2\big) z_{i-1,1}, \end{aligned} \tag{38}$$

where A_0 and B are given in (12), I_2 denotes the 2-dimensional identity matrix, and

$$E = \begin{bmatrix} 0 & 1 \\ -1 & 0 \end{bmatrix}, \quad F(\theta) = \begin{bmatrix} \cos(\theta) & -\sin(\theta) \\ \sin(\theta) & \cos(\theta) \end{bmatrix}. \tag{39}$$

Note that $c_{0,1} = 0$ and $d_{0,1} = v_{\mathrm{amp}}$; cf. (33).

When considering (34) for $j = 2$ and $j = 3$, the whole network becomes an LTI system with excitations $\tilde{h}_{i,1}^2$ and $\tilde{h}_{i,1}^3$, respectively. As $\tilde{h}_{i,1}^2$ only contains the frequency 2ω

while $\tilde{h}^3_{i,1}$ contains frequencies ω and 3ω, the corresponding steady states for $j=2$ and $j=3$ are in the form

$$\begin{aligned}
\tilde{h}_{i,2}(t) &= a_{i,2}\cos(2\omega t)+b_{i,2}\sin(2\omega t)\,,\\
\tilde{v}_{i,2}(t) &= c_{i,2}\cos(2\omega t)+d_{i,2}\sin(2\omega t)\,,\\
\tilde{h}_{i,3}(t) &= a_{i,3,1}\cos(\omega t)+b_{i,3,1}\sin(\omega t)\\
&\quad +a_{i,3,3}\cos(3\omega t)+b_{i,3,3}\cos(3\omega t)\,,\\
\tilde{v}_{i,3}(t) &= c_{i,3,1}\cos(\omega t)+d_{i,3,1}\sin(\omega t)\\
&\quad +c_{i,3,3}\cos(3\omega t)+d_{i,3,3}\cos(3\omega t)\,.
\end{aligned} \tag{40}$$

We also collect the coefficients in vectors as follows

$$\begin{aligned}
z_{i,2} &= [a_{i,2}\ b_{i,2}\ c_{i,2}\ d_{i,2}]^{\mathrm{T}}\,,\\
z_{i,3,k} &= [a_{i,3,k}\ b_{i,3,k}\ c_{i,3,k}\ d_{i,3,k}]^{\mathrm{T}}\,,\quad k=1\,,3\,,
\end{aligned} \tag{41}$$

cf. (36). Substituting (40) into (34) for $j=2$ and $j=3$ and solving for the coefficients yields

$$\begin{aligned}
z_{i,2} &= \big(C(2\omega)\big)^{-1}D_{i,2}\,,\\
z_{i,3,k} &= \big(C(k\omega)\big)^{-1}D_{i,3,k}\,,\quad k=1\,,3\,,
\end{aligned} \tag{42}$$

where the matrix C is defined in (38) and

$$\begin{aligned}
D_{i,2} &= \big(B\otimes F(2\omega\sigma)-A_0\otimes I_2\big)z_{i-1,2}+\alpha M(2\omega\sigma)J_i\,,\\
D_{i,3,k} &= \big(B\otimes F(k\omega\sigma)-A_0\otimes I_2\big)z_{i-1,3,k}+\alpha M(k\omega\sigma)K_{i,k}\,,
\end{aligned} \tag{43}$$

with

$$\begin{aligned}
M(\theta) &= \begin{bmatrix} \mathbf{0}_{2\times 2} & \mathbf{0}_{2\times 2}\\ \mathbf{0}_{2\times 2} & F(\theta)\end{bmatrix}\,,\\
J_i &= [0\,,\ 0\,,\ (a_{i,1}^2-b_{i,1}^2)/2\,,\ a_{i,1}b_{i,1}]^{\mathrm{T}}\,,\\
K_{i,1} &= [0\,,\ 0\,,\ \big(3a_{i,1}^3+3a_{i,1}b_{i,1}^2\big)/4\,,\ \big(3a_{i,1}^2b_{i,1}+3b_{i,1}^3\big)/4]^{\mathrm{T}}\,,\\
K_{i,3} &= [0\,,\ 0\,,\ \big(a_{i,1}^3-3a_{i,1}b_{i,1}^2\big)/4\,,\ \big(3a_{i,1}^2b_{i,1}-b_{i,1}^3\big)/4]^{\mathrm{T}}\,.
\end{aligned} \tag{44}$$

Substituting (35) and (40) into (32) results in the approximation of $\tilde{h}_{is}(t)$ and $\tilde{v}_{is}(t)$. Then, the CCC cascade is head-to-tail string stable if

$$\Upsilon_{n,0}(v_{\mathrm{amp}},\omega)=\|\tilde{v}_{ns}\|_\infty/\|\tilde{v}_0\|_\infty\le 1\,,\quad \forall\omega\ge 0\,, \tag{45}$$

cf. (6). Here, $\|\tilde{v}_0\|_\infty=v_{\mathrm{amp}}$ while $\|\tilde{v}_{ns}\|_\infty$ can be numerically obtained for $t\in[0,2\pi/\omega]$. Note that the amplification ratio $\Upsilon_{n,0}(v_{\mathrm{amp}},\omega)$ in (45) depends on both the disturbance amplitude and the frequency due to nonlinearities. This is different from the amplification ratio obtained using a linearized model (see, e.g., [4]), which only depends on the disturbance frequency. Therefore, the string stable domains obtained at nonlinear level may change as the disturbance amplitude varies.

IV. STABILITY DIAGRAMS AND SIMULATIONS

In this section, we consider a CCC cascade of 31 vehicles; see Fig. 2 with $n=30$. We assume that the communication delay is $\sigma=0.2$ [s] and the headways are bounded in the domain $\mathscr{D}=\{h:13\le h\le 27\}$. We remark that considering larger domain $\mathscr{D}$ leads to a smaller stable region in the plane of control gains. Since the stability conditions presented in this paper are sufficient for stability, the system may still be stable for states outside the domain $\mathscr{D}$. Stability diagrams are shown in Fig. 3 for disturbance amplitudes $v_{\mathrm{amp}}=1$ [m/s] and $v_{\mathrm{amp}}=6$ [m/s]. The plant stable domain (light gray) enclosed by red solid curves is obtained by (18). The blue solid boundary results from (45). Since plant stability is a precondition for string stability, the string stable domain (dark gray) is the overlap between the plant stable domain and the region enclosed by blue solid curve. Here, the domains enclosed by dashed-dotted red and blue curves are the plant and string stable domains obtained using the linearized model shown in [4], which do not change with the disturbance amplitude. Fig. 3(a) shows that the linear and the nonlinear string stable domains are similar when the disturbance amplitude is small, but the difference increases for large disturbance amplitudes; see Fig. 3(b).

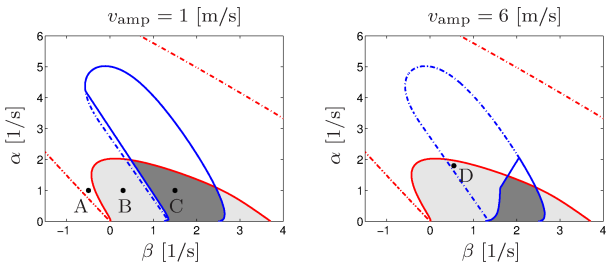

Fig. 3. Stability diagrams for different disturbance amplitudes as indicated. Nonlinearly plant stable domain (light gray) and string stable domain (dark gray) are enclosed by solid red and blue boundaries that result from (18) and (45), respectively. Linearly plant stable and string stable domains are enclosed by dashed-dotted red and blue curves, respectively.

To demonstrate the system performance, we select the points A–C in Fig. 3(a). The initial conditions are given by $h_i(t)\equiv 20$ [m] and $v_i(t)\equiv 20$ [m/s] for $i=1,\dots,30$ and $t\in[-\sigma,0]$. When evaluating plant stability, we assume constant speed of head vehicle $v_0(t)\equiv 22.5$ [m/s]. Simulations in Fig. 4(a,b) correspond to points A and B. Note that case A is plant unstable although it is in the linearly plant stable domain. This indicates that the linear stability of the equilibrium cannot ensure the stability of the nonlinear system for large perturbations. To investigate head-to-tail string stability, we assume sinusoidal disturbance on the speed of head vehicle $v_0(t)=22.5+v_{\mathrm{amp}}\sin(\omega t)$ where $v_{\mathrm{amp}}=1$ [m/s] and $\omega=0.8$ [rad/s]; cf. (5). The simulations in Fig. 4(c,d) indicate that case B is head-to-tail string unstable but head-to-tail string stability is achieved in case C. Fig. 4(c) also shows that the steady-state speed of tail vehicle is periodic with the same frequency as the speed of head vehicle.

For nonlinear systems, bistability may occur, indicating that the system is stable for small disturbances but loses stability for large disturbances. Here, we choose point D in Fig. 3(b) to demonstrate this phenomenon. We assume $v_0(t)=22.5+v_{\mathrm{amp}}\sin(\omega t)$ where $\omega=0.4$ [rad/s]; cf. (5). Simulations in Fig. 5(a,b) show that the system is string stable for $v_{\mathrm{amp}}=1$ [m/s] but string unstable for $v_{\mathrm{amp}}=6$ [m/s]. This indicates that the linear string stable domain is not applicable for large disturbances while it can be used

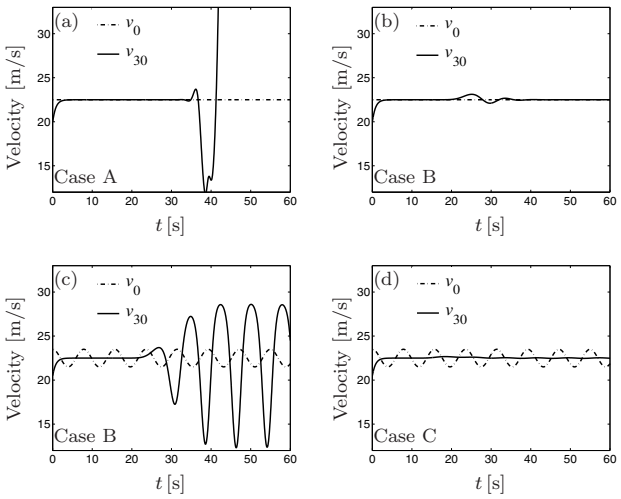

Fig. 4. Simulation results for CCC cascade. (a,b): cases A and B for plant stability. (c,d): cases B and C for string stability. Black dash-dotted and solid curves denote the speeds of the head and the tail vehicles, respectively.

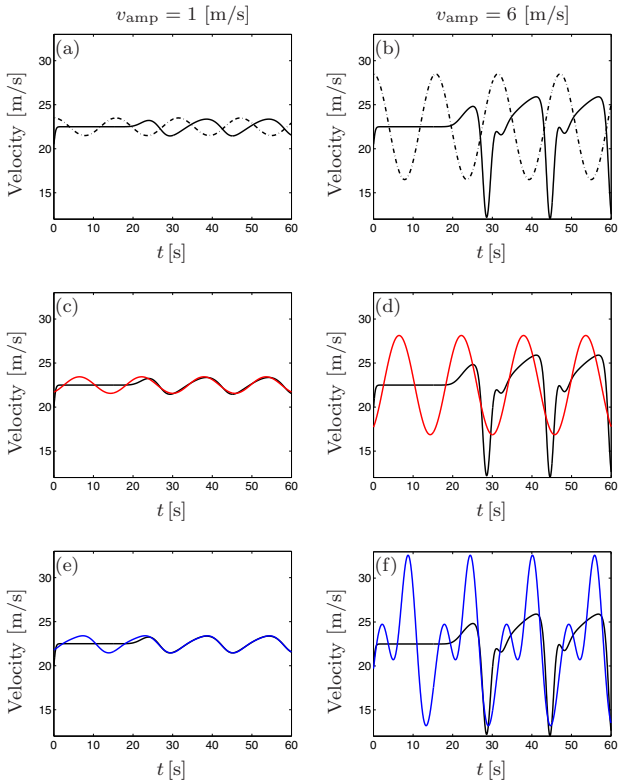

Fig. 5. Simulations and comparisons between simulation and approximations for $v_{\text{amp}} = 1$ [m/s] and $v_{\text{amp}} = 6$ [m/s], respectively. Black dash-dotted and black solid curves indicate the velocities of head vehicle and tail vehicle, respectively. Red and blue curves are used to denote linear and nonlinear approximations, respectively.

when disturbances are small. In Fig. 5(c–f), we compare the numerical simulations of the tail vehicle (black curve) with the corresponding linear approximation (red curve) and nonlinear approximation (blue curve). When $v_{\text{amp}} = 1$ [m/s], both linear and nonlinear approximations track the real steady state well; see Fig. 5(c,e). When $v_{\text{amp}} = 6$ [m/s], the error between the numerical simulation and the approximations becomes significant. However, compared with the linear approximation, the peak value of nonlinear approximation is much closer to the peak value of the real steady state; see Fig. 5(d,f). Since $\|\tilde{v}_{ns}\|_\infty$ determines the string stability, the nonlinear string stable domains in Fig. 3 can approximate the exact stable domain well for large disturbance amplitudes.

V. CONCLUSIONS

In this paper, we investigated the nonlinear dynamics of connected vehicle systems in presence of communication delays caused by intermittency and packet drops in vehicle-to-vehicle communication. Delay-dependent sufficient conditions for plant stability and head-to-tail string stability were derived based on the Lyapunov-Krasovskii theory. Simulations were conducted to validate the stability conditions for large disturbances. In the future, the present work will be extended by investigating effects of connectivity structures on the dynamics of heterogeneous vehicle networks.

REFERENCES

[1] V. Milanes, S. E. Shladover, J. Spring, C. Nowakowski, H. Kawazoe, and M. Nakamura, "Cooperative adaptive cruise control in real traffic situations," *IEEE Transactions on Intelligent Transportation Systems*, vol. 15, no. 1, pp. 296–305, 2014.

[2] A. Geiger, M. Lauer, F. Moosmann, B. Ranft, H. Rapp, C. Stiller, and J. Ziegler, "Team AnnieWAY's entry to the 2011 grand cooperative driving challenge," *IEEE Transactions on Intelligent Transportation Systems*, vol. 13, no. 3, pp. 1008–1017, 2012.

[3] J. Ploeg, B. T. M. Scheepers, E. van Nunen, N. van de Wouw, and H. Nijmeijer, "Design and experimental evaluation of cooperative adaptive cruise control," in *14th International IEEE Conference on Intelligent Transportation Systems (ITSC)*, 2011, pp. 260–265.

[4] L. Zhang and G. Orosz, "Designing network motifs in connected vehicle systems: delay effects and stability," in *Proceedings of the ASME Dynamic Systems and Control Conference*, no. DSCC2013-4081, 2013, p. V003T42A006.

[5] W. B. Qin, M. M. Gomez, and G. Orosz, "Stability analysis of connected cruise control with stochastic delays," in *American Control Conference*, 2014, pp. 5534–5539.

[6] J. I. Ge and G. Orosz, "Dynamics of connected vehicle systems with delayed acceleration feedback," *Transportation Research Part C*, vol. 46, pp. 46–64, 2014.

[7] G. Orosz, "Connected cruise control: modeling, delay effects, and nonlinear behavior," *Vehicle System Dynamics,*, p. submitted, 2014.

[8] P. Seiler, A. Pant, and K. Hedrick, "Disturbance propagation in vehicle strings," *IEEE Transactions on Automatic Control*, vol. 49, no. 10, pp. 1835–1842, 2004.

[9] M. R. Jovanovic and B. Bamieh, "On the ill-posedness of certain vehicular platoon control problems," *IEEE Transactions on Automatic Control*, vol. 50, no. 9, pp. 1307–1321, 2005.

[10] L. Zhang and G. Orosz, "Stability analysis of nonlinear connected vehicle systems," in *Proceedings of the ASME Dynamic Systems and Control Conference*, no. DSCC2014-6358, 2014, p. V001T10A006.

[11] G. Orosz, R. E. Wilson, and G. Stépán, "Traffic jams: dynamics and control," *Philosophical Transactions of the Royal Society A*, vol. 368, no. 1928, pp. 4455–4479, 2010.

[12] M. Krstic, *Delay compensation for nonlinear, adaptive and PDE systems*. New York, USA: Birkhäuser, 2009.